Cell Reports

Article

Yeast TIA1 coordinates with Npl3 to promote *ATG1* translation during starvation

Graphical abstract

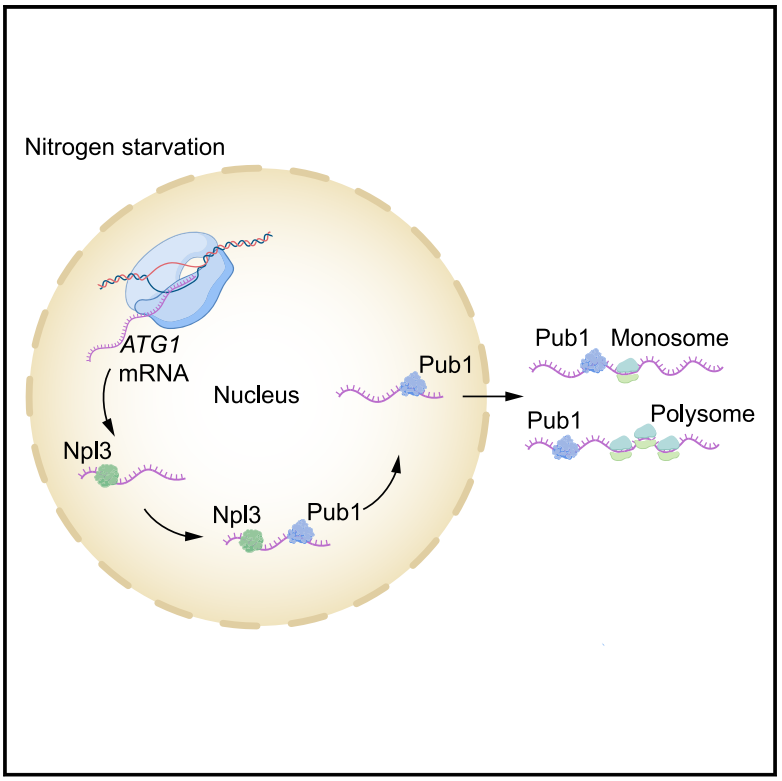

Authors

Shree Padma Metur, Xinxin Song, Sophie Mehta, ..., Zhangyuan Yin, Daolin Tang, Daniel J. Klionsky

Correspondence

klionsky@umich.edu

In brief

Metur et al. uncover functions for RNA-binding proteins, Npl3 and Pub1, as key regulators of *ATG1* mRNA translation and autophagy during nutrient starvation. They show that Npl3 and Pub1 coordinate to promote *ATG1* export, polysome recruitment, and subsequent translation to sustain autophagy levels required for survival during nutrient starvation.

Highlights

- Npl3 and Pub1 are post-transcriptional regulators of the *ATG1* transcript
- Pub1 facilitates *ATG1* translation by linking its export with the ribosomal machinery
- TIA1 promotes ULK1 protein expression and autophagy

Metur et al., 2025, Cell Reports *44*, 115316
February 25, 2025
https://doi.org/10.1016/j.celrep.2025.115316

CellPress

Cell Reports

CellPress
OPEN ACCESS

Article

Yeast TIA1 coordinates with Npl3 to promote *ATG1* translation during starvation

Shree Padma Metur,[1,2] Xinxin Song,[3] Sophie Mehta,[1,2] Dimitra Dialynaki,[1] Dibyendu Bhattacharyya,[1] Zhangyuan Yin,[1,2] Daolin Tang,[3] and Daniel J. Klionsky[1,2,4,*]

[1]Life Sciences Institute, University of Michigan, Ann Arbor, MI 48109-2216, USA
[2]Department of Molecular, Cellular and Developmental Biology, University of Michigan, Ann Arbor, MI 48109, USA
[3]Department of Surgery, University of Texas Southwestern Medical Center, Dallas, TX 75390, USA
[4]Lead contact
*Correspondence: klionsky@umich.edu
https://doi.org/10.1016/j.celrep.2025.115316

SUMMARY

Macroautophagy/autophagy is crucial for cell survival during nutrient starvation. Autophagy requires the coordinated function of several Atg proteins, including the Atg1 kinase, for efficient induction and execution. Recently, several RNA-binding proteins (RBPs) have been shown to post-transcriptionally regulate *ATG1*. However, a comprehensive understanding of autophagy regulation by RBPs via *ATG1* is yet to be elucidated. Here, we utilize an *in vitro* approach to identify RBPs that specifically interact with *ATG1* untranslated regions. We show that Npl3 and Pub1 interact with the *ATG1* 5′ and 3′ untranslated regions during nitrogen starvation. Furthermore, Npl3 and Pub1 coordinate to facilitate *ATG1* mRNA export to the cytoplasm and its subsequent interaction with the translational machinery. Significantly, in non-small cell lung cancer cell lines, mammalian Pub1, TIA1, also positively regulates ULK1 protein expression and autophagy during serum starvation. Overall, our study highlights the regulatory landscape that fine-tunes Atg1 protein expression to sustain autophagy during nutrient starvation.

INTRODUCTION

A fundamental challenge faced by all living organisms is adapting to ever-changing external environments, with fluctuations in nutrient availability being the most critical and ubiquitous of these changes.[1] In response to nutrient scarcity, cellular decisions strategically utilize available metabolic nutrients to ensure survival. This response is characterized by the upregulation of macroautophagy (hereafter, autophagy), a critical process that plays a central role in adapting to metabolic perturbations.[2]

Autophagy is an evolutionarily conserved catabolic mechanism in eukaryotes designed to maintain cellular homeostasis in response to changes in the nutrient composition of the external environment.[3] A characteristic feature of autophagy is the formation of double-membrane structures called phagophores, which engulf cytoplasmic cargo; the phagophores mature into autophagosomes that deliver the cargo to the vacuole for degradation.[4] Following degradation, metabolic building blocks are released to the cytosol, which mitigates the metabolic strain brought on by nutrient depletion, ensuring survival during periods of starvation.[5] Moreover, this mechanism is crucial for the clearance of damaged organelles and misfolded proteins, the accumulation of which has been shown to cause cancer, neurodegenerative diseases, and various metabolic disorders. Therefore, autophagy is not only an essential cytoprotective process that eliminates superfluous materials but also a key player in maintaining metabolic homeostasis and preventing the onset of various diseases.

Autophagy is primarily a degradative process and, therefore, must be fine-tuned to meet cellular requirements while avoiding unnecessary breakdown of the cytoplasm.[6] Therefore, autophagy is subject to regulation by a complex interplay of several nutrient responders that control its induction and execution. These nutrient responders act at multiple levels that upregulate autophagy by directly modulating the expression of essential autophagy genes at the level of both transcription and translation. While several studies have described the transcriptional regulation of autophagy, we are only now beginning to discover novel post-transcriptional and translational regulators of autophagy.[7]

Atg1/ULK1 is a crucial autophagy protein in yeast and mammalian cells; it is an essential Ser/Thr kinase for initiating autophagy and the only protein kinase among the core autophagy machinery that is required for autophagosome formation.[8] Immediately upon the induction of starvation-dependent autophagy, both *ATG1* mRNA and protein levels of Atg1 are upregulated.[9] However, during nitrogen starvation, global translation is downregulated. How *ATG1* transcripts escape this global repression still remains elusive. RNA-binding proteins (RBPs) are effective nutrient responders that link external nutrient cues with post-transcriptional regulation.[10] Recent studies have identified several RBPs interacting with *ATG1* mRNA, influencing its stability and association with translation

initiation factors. These interactions have significant implications for autophagy regulation.[9,11,12] Furthermore, these studies allude to the intricate network of interactions involving *ATG1* mRNA, hinting at layers of potential regulatory control that span the multiple stages of its biosynthesis and usage. Therefore, we hypothesized the presence of a dynamic RBP interactome with *ATG1* transcripts in response to changing nutrient cues that regulate Atg1 protein expression, uncovering potential regulators of autophagy.

To comprehensively understand the nutrient-responsive regulatory paradigm of *ATG1* transcripts, we profiled the RNA-binding proteome of the *ATG1* 5′ untranslated region (UTR) and 3′ UTR in response to nutrient-rich and nitrogen-starvation conditions.[9] We identified Npl3 and Pub1 as interacting partners of the *ATG1* transcript at the 5′ UTR and 3′ UTR, respectively and also showed that they are positive regulators of autophagy. We further characterized the role of Npl3 in conjunction with Pub1, a stress granule protein, in regulating *ATG1* mRNA export and ribosome association to promote its translation during nitrogen starvation. Intriguingly, the mammalian homolog of Pub1, TIA1, also positively regulates ULK1 expression at the post-transcriptional level, thereby promoting autophagy in response to nutrient starvation. This finding not only underscores the evolutionary importance of this regulatory pathway but also highlights the potential for translatability of this mechanism. Taken together, we provide insights into the intricate network of protein interaction linked with *ATG1* mRNA that governs the expression of the Atg1 protein and, thus, autophagy.

RESULTS

An *in vitro* interactome capture reveals several new binding partners of *ATG1* mRNA

To identify potential RBPs involved in autophagy regulation at the level of the *ATG1* transcript, we performed an *in vitro* transcribed *ATG1* 5′ UTR RNA affinity isolation followed by western blot and proteomics to identify interactors in nitrogen-rich (+N) and nitrogen-limited (−N) conditions (Figure 1A). We verified through western blot that Dhh1 and Ded1, known interactors with the *ATG1* 5′ UTR, were enriched only in the presence of labeled *ATG1* 5′ UTR RNA (Figure S1A). Proteomics profiling of the affinity isolate identified previously known interacting proteins of the *ATG1* 5′ UTR, such as Eap1 and Psp2, under nitrogen-starvation conditions (Figure S1B), further validating the utility of this method to identify potential RBPs that could regulate autophagy at the level of *ATG1* mRNA. We identified 13 RBPs that were significantly enriched on the *ATG1* 5′ UTR during nitrogen starvation relative to rich medium (Figure 1B). Out of the 13, we decided to test three non-essential proteins with a previously unknown role in regulating autophagy (Table S1 and Data S1). Accordingly, we created genomic deletion strains of *SRO9*, *NPL3*, and *MLF3* and tested them for effects on Atg1 protein expression using immunoblotting (Figure 1C). We found that *NPL3* deletion severely abrogated the upregulation in Atg1 protein levels relative to the wild-type (WT) strain only under nitrogen-starvation (−N) conditions. Interestingly, *npl3* deletion did not affect Atg1 protein levels under growing conditions (+N), suggesting a potential role of Npl3 in regulating Atg1 expression in response to nitrogen starvation. In contrast, the other two deletion strains caused no obvious change in Atg1 levels relative to the WT.

Npl3 is a novel regulator of Atg1 protein expression and autophagy

To confirm that Npl3 does indeed bind to the *ATG1* transcript, we performed an Npl3 immunoprecipitation followed by RT-qPCR to measure *ATG1* transcript levels and determine whether the transcript was enriched specifically in nitrogen-starvation medium relative to nitrogen-rich medium. Our results show that Npl3 bound to both the 5′ UTR (−290) and the coding region (+35) but not the 3′ UTR (Figure 1D), revealing that Npl3 is indeed an interactor with the *ATG1* 5′ UTR during nitrogen starvation. We hypothesized that this interaction is crucial for the upregulation of Atg1 protein levels during nitrogen-starvation-induced autophagy. To rule out the possibility that increased protein turnover results in lowered Atg1 protein levels in Npl3 mutants, we performed a cycloheximide (CHX) chase assay in which Atg1 protein levels were allowed to accumulate during 6 h of nitrogen starvation, following which CHX was added. The Atg1 protein levels were then chased in nitrogen-starvation medium for another 1 h and 2 h and measured by immunoblotting using an Atg1-specific antibody. The results show that the turnover of Atg1 protein levels in both WT and *npl3Δ* strains was similar and, therefore, the regulation was upstream of protein degradation (Figures 1E and 1F). Next, we measured the mRNA levels of the *ATG1* transcript in WT and *npl3Δ* cells to assess whether the lowered amount of Atg1 protein is due to a decrease in *ATG1* mRNA levels and, therefore, a form of transcriptional regulation by Npl3. However, both WT and *npl3Δ* strains had similar levels of *ATG1* mRNA transcript in both +N and −N conditions (Figure 1G), suggesting that Npl3 regulates Atg1 protein levels at the post-transcriptional/translational level, only in response to nitrogen starvation.

The decline in Atg1 protein levels upon ablation of the *NPL3* gene led us to test whether the decrease affects autophagy activity. Toward this end, we tested GFP-Atg8 processing. Atg8, or GFP-tagged Atg8, is attached to both sides of the phagophore via conjugation to phosphatidylethanolamine. After autophagosome maturation, Atg8/GFP-Atg8 is removed from the autophagosome outer membrane and recycled; in contrast, the protein on the inner surface is delivered to the vacuole after fusion with the autophagosome.[13] Atg8 is degraded within the vacuole lumen, whereas GFP is relatively stable and accumulates within the vacuole. Thus, the generation of free GFP is an indication of autophagy activity. We determined that deletion of *NPL3* resulted in decreased GFP-Atg8 processing after 6 h of nitrogen starvation and, therefore, a lower level of autophagy activity (Figures 1H and 1I). To assess whether the lowered autophagic activity is primarily due to a decrease in Atg1 protein levels, we placed the *ATG1* open reading frame (ORF) under an inducible promoter to overexpress the Atg1 protein levels and tested whether this overexpression could rescue the autophagy defect measured by GFP-Atg8 processing. Overexpression of Atg1 partially rescued the autophagy defect seen in *npl3Δ* cells, suggesting that, while *ATG1* is a key target of Npl3, there are likely

CellPress
OPEN ACCESS

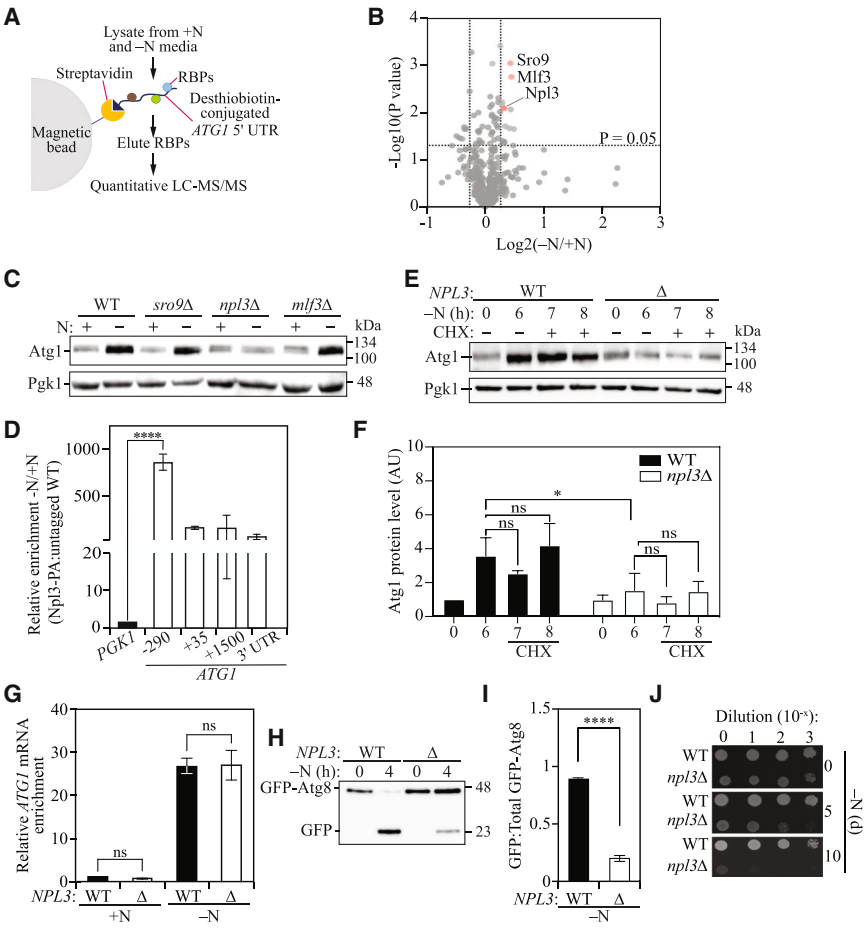

Figure 1. Exploring *ATG1*-RBP interactions reveals Npl3 as a novel regulator of autophagy

(A) Schematic of *in vitro ATG1* mRNA interactome capture. Lysates from rich medium (+N) and nitrogen starvation medium (−N) were incubated with streptavidin beads conjugated with desthiobiotin-tagged *ATG1* 5′ UTR. The beads were washed, and the RBPs bound to the beads were identified by mass spectrometry.

(B) RBP-5′ UTR interaction reveals novel binding partners of *ATG1*: volcano plot of RBPs interacting with the *ATG1* 5′ UTR in −N compared to +N. Results from three biological replicates are plotted. Student's t test between the −N and +N conditions was performed to identify statistically significant enrichments.

(C) Npl3 is a novel regulator of Atg1 expression. WT (WLY176) and RBP deletion strains were grown in +N medium and shifted to −N for 6 h, following which lysates were analyzed by immunoblotting to measure Atg1 protein levels using Atg1-specific antibody. Pgk1 was used as a loading control.

(D) RNA immunoprecipitation confirms Npl3 interaction with *ATG1* is specific to −N conditions. Lysates of Npl3 tagged with PA (YZY312) from +N and −N was affinity isolated using IgG Sepharose beads, and bound mRNA was extracted and quantified by RT-qPCR. The region of interaction was determined using primers specific to different regions of the *ATG1* mRNA as indicated. *PGK1* was used as an internal control, and an untagged strain (SEY6210) was used for normalization. Data represent three independent biological replicates showing mean ± SD. One-way ANOVA was used to determine statistical significance. ****$p < 0.001$.

(E) The *npl3* deletion does not increase turnover of the Atg1 protein. WT (WLY176) and *npl3Δ* (SPY77) cells were grown in +N and transferred to −N for 6 h and treated thereafter with cycloheximide (CHX). Following treatment, cells were harvested at the indicated time points. Atg1 protein levels were measured by immunoblotting. Pgk1 was used as a loading control.

(F) Quantification of (E), representing data from two biological replicates, mean ± SD. Two-way ANOVA was used to determine statistical significance. *$p = 0.0124$; ns, not significant.

(G) Npl3 does not regulate *ATG1* at the level of transcription. WT (WLY176) and *npl3Δ* (SPY77) strains were subjected to nitrogen starvation for 6 h, after which total RNA was extracted and cDNA synthesized. RT-qPCR was performed to quantify the abundance of *ATG1* mRNA. Data represent three biological replicates. Student's t test was performed to determine statistical significance. ns, not significant.

(H) Ablation of *NPL3* results in reduced autophagic flux. WT (JMY347) and *npl3Δ* (YZY311) cells expressing genomically tagged Atg8-GFP were starved for nitrogen, harvested after 4 h, and assessed by immunoblotting.

(I) Quantification of (H). The ratio of the free GFP to total GFP is a measure of autophagic flux. Data are representative of three biological replicates, showing mean ± SD. Student's t test was performed to determine the statistical significance. ****$p < 0.0001$.

(J) Loss of Npl3 leads to reduced cell survival during nitrogen starvation: WT (SEY6210) and *npl3Δ* (SPY77) cells were grown in +N and starved for the indicated time points. The indicated dilutions were grown on YPD plates for 2 days at 30°C.

other targets that lead to the autophagy defect (Figures S1C and S1D).

Finally, autophagy is required for yeast cell viability during starvation; autophagy mutants display decreased viability under starvation conditions.[14] Thus, resistance to starvation is another measure of functional autophagy. The *npl3* deletion resulted in decreased cellular viability during long-term starvation compared to the WT strain (Figure 1J), although we did note a slight growth defect in growing conditions. This result suggests that Npl3 is an essential factor required for survival during nitrogen starvation and that it primarily acts by promoting Atg1 protein levels and autophagy activity.

Npl3 regulates Atg1 expression and autophagy in an RRM-dependent manner

Npl3 belongs to a family of serine-arginine/SR proteins well studied for its role in mRNA splicing. Npl3 has also been implicated in various stages of gene expression such as transcription elongation, termination, and mRNA splicing. The *ATG1* transcript in *Saccharomyces cerevisiae* does not contain any introns and because the depletion of *NPL3* did not affect *ATG1* mRNA levels but only the Atg1 protein level, we asked whether (1) export and (2) translational efficiency of *ATG1* mRNA was affected. To test whether there was a defect in mRNA export, we isolated total mRNA from nuclear and cytoplasmic fractions from WT and

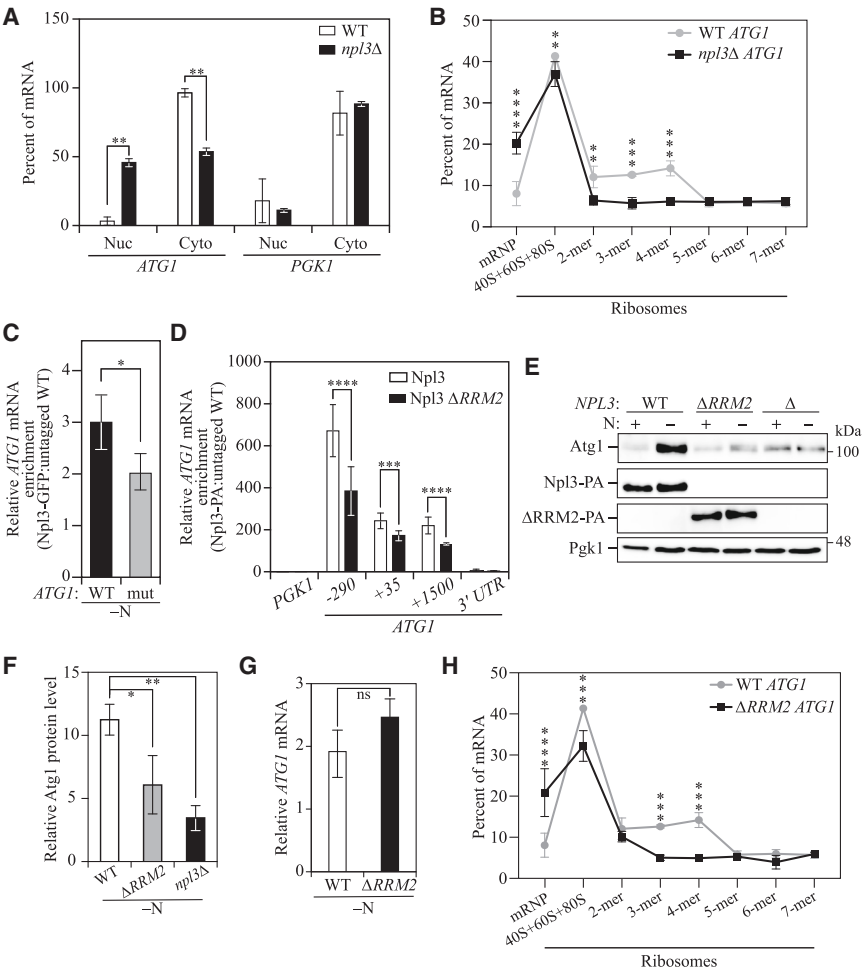

Figure 2. Npl3 promotes *ATG1* translation and autophagy through an RRM-motif-dependent mechanism

(A) Npl3 is required for export of *ATG1* mRNA. WT (SEY6210) and *npl3Δ* (SPY77) strains were starved of nitrogen for 4 h and fractionated to obtain nuclear and cytoplasmic fractions; 20 pg of spike-in control RNA was then added, and total RNA was extracted. RT-qPCR was performed to quantify the percentage of *ATG1* mRNA in the two fractions. *PGK1* was used as a control RNA, showing the specificity of this regulation. The spike-in RNA was used for normalization. Data represent three biological replicates, showing mean ± SD. Two-way ANOVA was performed to determine the statistical significance. $^{**}p = 0.0388$.

(B) Polysome recruitment onto *ATG1* mRNA is reduced when *NPL3* is deleted. WT (SEY6210) and *npl3Δ* (SPY077) cells were subjected to nitrogen starvation. Lysates were fractionated in a sucrose gradient, and the abundance of *ATG1* transcript was analyzed by RT-qPCR. Data represent two independent biological replicates, showing mean ± SD. Two-way ANOVA was performed to determine the statistical significance. $^{****}p < 0.0001$, $^{***}p < 0.0005$, $^{**}p < 0.01$.

(C) Npl3 targets the 5′ UTR of the *ATG1* transcript. Npl3-GFP-tagged strains with the WT *ATG1* promoter (SPY113) and in an *ATG1* mutant where the endogenous promoter is switched to the 5′ UTR of *ATG7* were subjected to nitrogen starvation for 6 h, and lysates collected were utilized to perform RNA immunoprecipitation. The abundance of the +35 fragment of *ATG1* mRNA was quantified to determine the importance of the 5′ UTR in enabling binding of *ATG1* with Npl3. Data represent two biological replicates, showing mean ± SD. A t test was performed to determine the statistical significance. $^{*}p = 0.0315$.

(D) Npl3 interacts with *ATG1* in an RRM2-dependent manner. RNA immunoprecipitation of WT (untagged, SEY6210), Npl3-PA (SPY060), and Npl3 ΔRRM2-PA (SPY062) was performed to quantify the abundance of *ATG1* mRNA interaction during nitrogen starvation. Data represent three biological replicates, showing mean ± SD. Two-way ANOVA was performed to determine statistical significance. $^{****}p < 0.0001$, $^{***}p = 0.0001$.

(E) The Npl3 RRM2 is required for upregulation of Atg1 protein during nitrogen starvation. WT (SEY6210), Npl3 ΔRRM2 (SPY060), and *npl3Δ* (SPY077) strains were subjected to nitrogen starvation for 6 h, and Atg1 protein levels were determined by immunoblotting. Pgk1 was used as a loading control.

(F) Quantification of (D). Two-way ANOVA was performed to determine statistical significance. $^{**}p = 0.0043$, $^{*}p = 0.0239$.

(G) Npl3 RRM2 truncation does not affect *ATG1* mRNA transcription. WT (SEY6210) and Npl3 ΔRRM2 (SPY060) cells were subjected to nitrogen starvation for 4 h and the abundance of *ATG1* mRNA determined. Student's t test was performed to determine statistical significance. ns, not significant.

(H) Polysome profiling shows that *ATG1* mRNA localization in cells expressing the Npl3 RRM2 deletion phenocopies *npl3Δ* during nitrogen starvation. *ATG1* mRNA abundance in different polysome fractions was quantified in the WT (SEY6210) and Npl3 ΔRRM2 strains. The data for the WT strain (SEY6210) are the same as in (B). Two-way ANOVA was performed to determine the statistical significance. $^{****}p < 0.0001$, $^{***}p < 0.001$.

npl3Δ cells after nitrogen starvation and measured the percentage of *ATG1* mRNA. The percentage of *ATG1* mRNA in the nuclear fraction was significantly higher in *npl3Δ* cells compared to the WT, whereas there was no significant difference seen with *PGK1*, suggesting a specific defect in *ATG1* mRNA export (Figure 2A).

For this defect to subsequently affect Atg1 protein expression, we hypothesized that the translational efficiency of the transcript should be affected in *npl3Δ* cells. Accordingly, we assessed the translational efficiency by measuring ribosome occupancy of *ATG1* mRNA during nitrogen starvation, carrying out polysome profiling of WT and *npl3Δ* cells followed by RT-qPCR to determine the localization of the transcript in free and ribosome-bound fractions. The resulting polysome profiles showed a negligible increase in the 60S and 80S fractions; however, there was no significant change in the polysome fraction, suggesting that the global translation remained unaffected in *npl3Δ* cells during nitrogen starvation (Figure S2A). Higher translational efficiency is a factor of higher ribosome occupancy, which localizes the transcript in the heavier polysome fractions. *ATG1* has high ribosome occupancy in WT cells during nitrogen starvation, as evidenced by the recruitment of two or more ribosomes on the transcript (Figure 2B). Furthermore, almost 40% of *ATG1* mRNA was occupied by one ribosome, suggesting the importance of

monosomes in translating stress-responsive genes.[15,16] In contrast, *npl3Δ* cells had a significant decrease in the abundance of *ATG1* mRNA in the polysome fraction compared to the WT, where two or more ribosomes occupy the transcript. There was a modest yet significant decrease in monosome loading and a proportional increase in the mRNA in the free mRNA-protein complexes (mRNPs) fraction in the *npl3Δ* strain, suggesting that depletion of *NPL3* reduced the ribosome loading onto the *ATG1* transcript; this effect was exacerbated in the polysome fractions. In contrast, the localization of the control mRNA, *PGK1*, was not drastically different in the mutant cells in the polysome fraction, with a modest decrease in the monosome and the free mRNP fractions (Figure S2B). However, the total protein levels of Pgk1 were not affected in *npl3Δ* cells, suggesting that this difference in *PGK1* localization in the various ribosome fractions had no effect on the total protein translation. Together, our data suggest that a decrease in Atg1 protein levels upon *npl3* deletion is due a deficiency in *ATG1* mRNA export and, therefore, a subsequent decrease in ribosome accessibility of the *ATG1* transcript.

Npl3 is an RBP with three potential RNA-binding motifs: two RNA recognition motifs (RRMs) and a C-terminal arginine-serine/RS domain containing an Arg-Gly-Gly (RGG) domain.[17] Genetic interactions analyzing the RNA recognition mechanism of Npl3 highlight the role of RRM1 during chromatin remodeling, while RRM2 might be linked to the regulation of a specific transcript.[18] Furthermore, RRM2 recognizes a 5′-GNGG-3′ motif, which is present in the 5′ UTR of *ATG1* starting at position 65 (Figure S2C). To test whether this motif had played a role in the interaction between Npl3 and the *ATG1* transcript, we constructed a strain wherein the 5′ UTR of the *ATG1* ORF was switched with the 5′ UTR of *ATG7*, the transcript of which is not a target of Npl3. Using this strain, we performed RNA immunoprecipitation with GFP-tagged Npl3 in WT and Atg1 mutant strains and measured the interaction of the +35 fragment of *ATG1*. Removal of the 5′ UTR significantly reduced the interaction with the coding region of the *ATG1* transcript, suggesting that Npl3 directly targets the 5′ UTR of *ATG1* (Figure 2C). Furthermore, we sought to determine whether Npl3 interacted with *ATG1* via its RRM2 domain. We deleted the Npl3 residues between 200 and 275 and first tested whether this affected the stability of the protein itself. We found that the truncation had no effect on the total protein stability compared to WT in both +N and −N conditions (Figure S2D); however, we found a modest but significant increase in total protein levels after 6 h of nitrogen starvation compared to growing conditions (Figures S2E and S2F). Next, we tested the effect of this truncation on *ATG1* interaction and Atg1 protein levels. We performed RNA immunoprecipitation with protein A (PA)-tagged WT Npl3 and Npl3 ΔRRM2 and analyzed the interaction with *ATG1* transcript fragments by RT-qPCR. Deleting RRM2 led to a significant reduction in *ATG1* mRNA enrichment compared to WT Npl3 (Figure 2D). Next, we tested the effect of deleting RRM2 on Atg1 protein levels using immunoblotting. Compared to the WT, the ΔRRM2 mutant showed significantly reduced Atg1 protein levels (Figures 2E and 2F). In contrast, *ATG1* mRNA levels remained unchanged (Figure 2G), suggesting that the RRM2 motif is essential for Npl3 to promote Atg1 protein expression but not for *ATG1* transcription. Finally, we asked whether this reduced binding in the ΔRRM2 mutant led to reduced accessibility for ribosome recruitment on the *ATG1* transcript. Indeed, the recruitment of both monosomes and polysomes on the *ATG1* transcript was significantly reduced in ΔRRM2 mutants compared to the WT, with a proportional increase in the percentage of *ATG1* in the free mRNP fraction (Figure 2G).

When the global translational status was profiled, we noticed a modest decrease in polysomes in the ΔRRM2 mutant during nitrogen starvation (Figure S2F), suggesting potential functional redundancy that may compensate for the loss of the complete protein (i.e., *npl3Δ*) but not for the RRM2 deletion alone, and further suggesting a weak dominant negative effect of the ΔRRM2 protein, wherein the truncated version of the protein interferes with normal cellular processes, possibly by disrupting interactions or functions typically associated with the full-length protein. Additionally, compared to WT, the control mRNA *PGK1* had a similar effect on the monosome and the free mRNP fractions but had no effect on polysomes (Figure S2G). Minor differences in *PGK1* localization did not manifest as differences in total Pgk1 protein levels, suggesting that polysome-binding-state differences for *PGK1* mRNA in the mutant had no effect on the final translation of the protein. These results suggest that Npl3 interacts with *ATG1* mRNA in an RRM2-dependent manner, and this interaction is necessary for the export and the subsequent recruitment of ribosomes and, thus, translational upregulation of Atg1 during nitrogen starvation. Taking the data together, we have identified Npl3 as a novel post-transcriptional regulator of *ATG1* mRNA during nitrogen starvation.

Pub1 promotes the translation of *ATG1* mRNA and autophagy

Having mapped the interaction network of the *ATG1* 5′ UTR, we were interested in analyzing the 3′ UTR. The *ATG1* 3′ UTR region binds to the Pat1-Lsm complex that protects the transcript from decay.[19] Specific RBP-3′ UTR interactions also influence association with translational machinery and ribosome components.[20] We employed the mRNA affinity-isolation approach followed by a proteomics analysis utilizing the labeled 3′ UTR of the *ATG1* transcript. Proteomics identification revealed that the *ATG1* 3′ UTR interacted with the 5′-3′ exonuclease Xrn1, previously shown to regulate Atg1 and autophagy[21] (Figure 3A). In addition, we found that the Npl3-interacting protein Gbp2, involved with the nuclear export of transcripts, also associated with *ATG1*. Hrb1, a paralog of Gbp2, was similarly identified as an interactor of the *ATG1* 3′ UTR (Data S2).[22] Furthermore, we identified ribosome component Rps27a, suggesting the crucial role of the 3′ UTR in regulating *ATG1* mRNA stability, export, and translation (Data S2).

The stress granule core protein Pub1 was also identified as interacting with the 3′ UTR of *ATG1* during nitrogen starvation (Figure 3A). Pub1 has not previously been implicated in autophagy, and therefore we were curious as to the significance of the Pub1 interaction with *ATG1* mRNA. To confirm this interaction, we immunoprecipitated Pub1-superfolder GFP (sfGFP) expressed from a plasmid, and tested whether it interacted with *ATG1* mRNA. We found significant enrichment of the *ATG1* 3′ UTR with additional binding in the 5′ UTR, suggesting that Pub1 indeed interacted with *ATG1* during nitrogen starvation (Figure 3B).

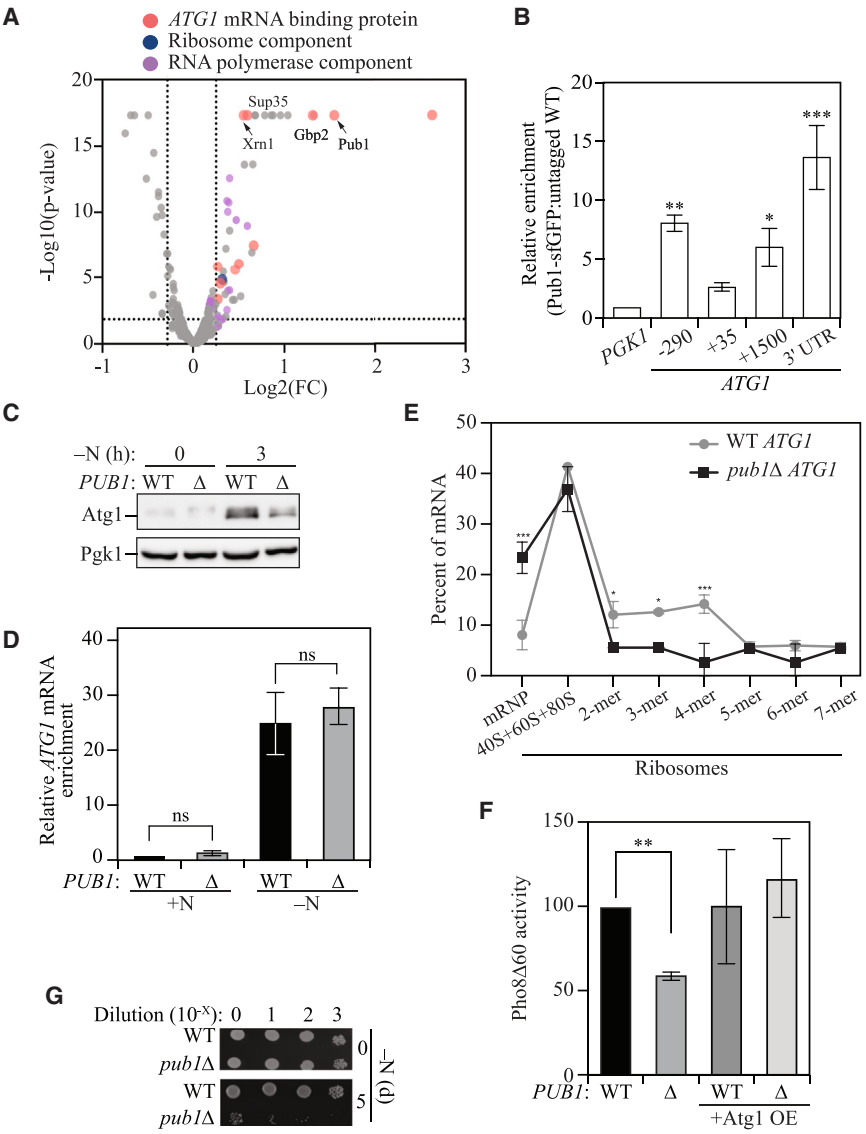

Figure 3. Pub1 promotes the translation of *ATG1* mRNA and autophagy

(A) An analysis of the *ATG1* 3′ UTR interaction network reveals novel interactors: volcano plot showing RBPs interacting with the *ATG1* 3′ UTR compared to *PGK1* as a control. The data show Npl3 interacting partners such as the previously identified Gbp2 and novel *ATG1* binding partners such as Xrn1 and Pub1 (highlighted in salmon). Data represent two independent biological replicates, showing mean ± SD. Student's t test was performed to determine statistical significance. *p* values above 0.05 were considered significant. FC, fold change.

(B) Pub1 interacts with the 3′ UTR of *ATG1* during nitrogen starvation. Pub1-sfGFP was expressed using a centromeric plasmid in a WT (SEY6210) strain and subjected to RNA immunoprecipitation following nitrogen starvation for 4 h. *ATG1* mRNA bound to Pub1 was quantified through RT-qPCR using primers specific to different regions on the transcript. Data represent two independent biological replicates, showing mean ± SD. One-way ANOVA was performed to determine statistical significance. ****p = 0.0003, **p = 0.0043, *p = 0.0164.

(C) Loss of Pub1 reduces Atg1 protein expression. WT (WLY176) and *pub1Δ* (SPY006) strains were subjected to nitrogen starvation for 3 h, and Atg1 protein levels were determined by immunoblotting. Pgk1 was used as a loading control.

(D) Loss of Pub1 does not affect *ATG1* transcription. WT (WLY176) and *pub1Δ* (SPY006) cells were subjected to nitrogen starvation for 3 h, and the abundance of *ATG1* mRNA was determined by RT-qPCR. Data represent three independent biological replicates, showing mean ± SD. Student's t test was performed to determine statistical significance. ns, not significant.

(E) Pub1 recruits polysomes onto the *ATG1* transcript during nitrogen starvation. WT (SEY6210) and *pub1Δ* (SPY006) strains were subjected to nitrogen starvation for 3 h, and the abundance of *ATG1* transcript in the different polysome fractions was determined using RT-qPCR. The data for the WT strain (SEY6210) are the same as in Figure 2B. Data are representative of two independent biological replicates, showing mean ± SD. Two-way ANOVA was used to determine statistical significance. ***p = 0.0004, **p = 0.0022, *p < 0.05.

(F) Pub1 is a positive regulator of autophagy during nitrogen starvation. WT (WLY176) and *pub1Δ* (SPY006) strains were subjected to nitrogen starvation for 4 h and assayed to determine Pho8Δ60 activity. WT and *pub1Δ* strains were transformed with a plasmid overexpressing *ATG1* under the control of the copper (*CUP1*) promoter. Overexpression of *ATG1* rescues the autophagy defect in *pub1Δ* cells. Data represent three independent biological replicates, showing mean ± SD. One-way ANOVA was performed to determine statistical significance. **p < 0.0067.

(G) Loss of Pub1 reduces viability during long-term nitrogen starvation. WT (WLY176) and *pub1Δ* (SPY006) strains were subjected to nitrogen starvation for the indicated times, and the indicated dilutions were spotted on YPD plates and grown for 3 days at 30°C.

As an interactor of the *ATG1* 3′ UTR, we next asked whether Pub1 regulates the expression of Atg1. From immunoblot analysis, we determined that *pub1Δ* cells did not upregulate Atg1 protein levels compared to the WT during nitrogen starvation (Figure 3C). However, the transcript levels of *ATG1* remained similar to those of WT under both growing conditions and during nitrogen starvation (Figure 3D). This result suggests that Pub1, similar to Npl3, regulates *ATG1* at the post-transcriptional level in response to nitrogen starvation. To confirm this hypothesis, we performed polysome profiling and analyzed the distribution of *ATG1* transcript in the different polysome fractions during nitrogen starvation, as we did for the *npl3Δ* strain. The polysome profiles confirmed that *pub1* deletion did not significantly affect the global translation during starvation (Figure S3A). However, *pub1* deletion did significantly reduce the localization of *ATG1* transcript in the polysome fractions, with a significant increase in the free mRNP fraction, suggesting a failure to recruit polysomes in the absence of Pub1, leading to reduced Atg1 protein levels during nitrogen starvation (Figure 3E).

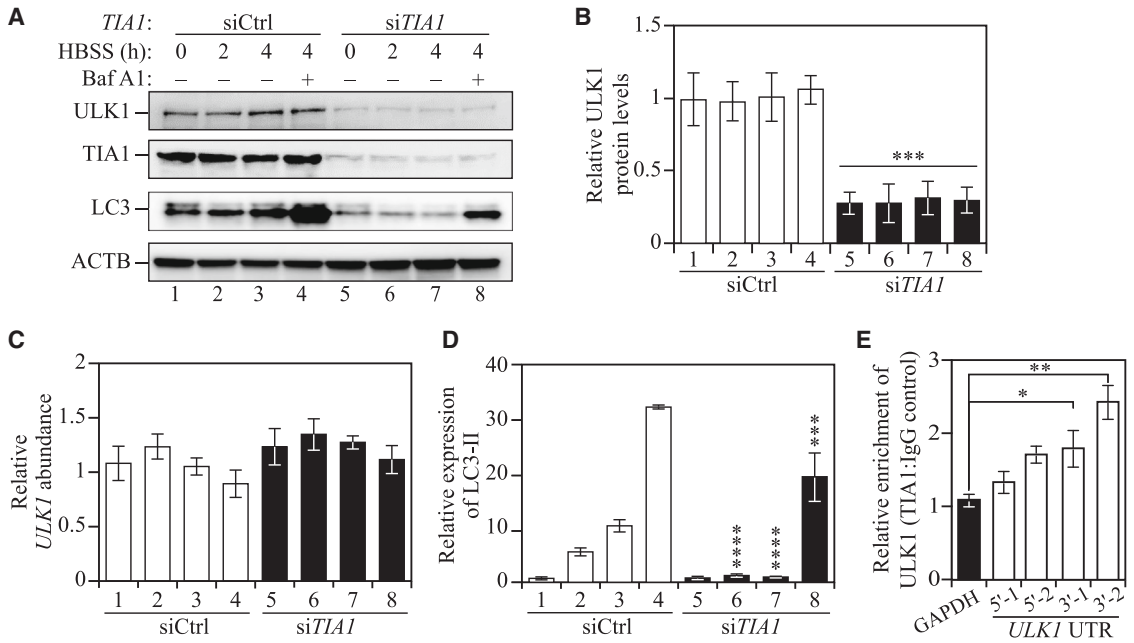

Figure 4. TIA1 promotes ULK1 protein expression and autophagy during nutrient starvation

(A) Loss of TIA1 reduces ULK1 protein expression and autophagy. Calu-1 cells transfected with either siRNA (control) or siRNA specific to *TIA1* were subjected to serum starvation for the indicated times with or without treatment with bafilomycin A_1. Cells were harvested after the indicated times and protein levels of ULK1, TIA1, and LC3 determined by immunoblotting. ACTB was used as a loading control.

(B) Quantification of ULK1 protein levels in (A). Data represent three independent biological replicates, showing mean ± SD. ****$p < 0.001$.

(C) TIA1 knockdown does not affect *ULK1* transcription. Total RNA was extracted from cells harvested under the conditions indicated in (A), and *ULK1* mRNA abundance was determined by RT-qPCR. *GAPDH* was used as a control. Data represent three independent biological replicates.

(D) Quantification of LC3-II levels in (A). Data represent three independent biological replicates, showing mean ± SD. two-way ANOVA was used to determine statistical significance. ****$p < 0.01$, ***$p < 0.05$.

(E) TIA1 binds to the 3′ UTR of *ULK1*. RNA immunoprecipitation was performed using TIA1-specific antibody, and the mRNA bound to the protein was quantified by RT-qPCR using two primers spanning different regions in the 5′ UTR and 3′ UTR. Data represent three independent biological replicates, showing mean ± SD. One-way ANOVA was performed to determine statistical significance. **$p = 0.0013$, *$p = 0.0358$.

In contrast, the control RNA *PGK1* did not show a drastic change in localization compared to the WT in the polysome fraction, in line with the fact that Pgk1 protein levels were not affected by *pub1* deletion (Figure S3B). The difference in *ATG1* translation and, therefore, Atg1 protein expression resulted in a difference in autophagy activity as measured by Pho8Δ60 activity (Figure 3F), an enzymatic assay that monitors autophagic flux.[23] Similarly, *pub1* deletion resulted in a significant difference in GFP-Atg8 processing and free GFP generation, albeit there was a significant difference in total GFP-Atg8 production between WT and *pub1Δ* (Figures S3C and S3D). When we overexpressed *ATG1* under an inducible promoter, the autophagy defect was almost completely rescued, suggesting that the autophagy defect in *pub1Δ* was primarily due to a deficiency in Atg1 protein levels (Figures 3F, S3C, and S3D). Finally, *pub1* deletion drastically reduced the viability of the cells during long-term starvation, providing insights into the critical role of Pub1 in ensuring cell survival during nutrition limitation (Figure 3G).

TIA1 promotes ULK1 expression and autophagy

To explore the conservation of the role of Pub1, a protein we have shown here to regulate Atg1 expression, we studied the capacity of TIA1, its mammalian counterpart, to influence ULK1 (a homolog of Atg1) protein expression. We used a non-small cell lung cancer cell line, Calu-1, to test the effect of TIA1 on ULK1 levels and autophagy. We found that the knockdown of TIA1 led to a reduction in protein levels of ULK1 in both the presence and absence of serum (Figures 4A and 4B) Crucially, stable knockdown of TIA1 using small interfering RNA (siRNA) had no effect on the transcript levels of *ULK1*, suggesting post-transcriptional regulation (Figure 4C). Next, we analyzed MAP1LC3B/LC3B-II levels using immunoblotting, which showed a consistent decrease post knockdown (KD) of TIA1 following serum starvation (Figures 4A and 4D). Treatment with bafilomycin A_1 blocks a late stage of autophagy and resulted in a substantial increase in ULK1 in the WT cells. In contrast, this treatment resulted in a significantly reduced accumulation of LC3B-II in TIA1 KD cells, indicating the reduction of autophagy in these cells as a result of lowered ULK1 levels (Figure 4D). Finally, we investigated whether TIA1 directly interacted with *ULK1* mRNA. Indeed, TIA1 showed significant enrichment at the 3′ UTR of *ULK1*, similar to Pub1 (Figure 4E). Taken together, these results indicate that TIA1 plays a significant role in regulating ULK1 expression and autophagy, emphasizing the conserved nature of the regulation at the 3′ UTR of both *ATG1* and *ULK1* via Pub1 and TIA1, respectively.

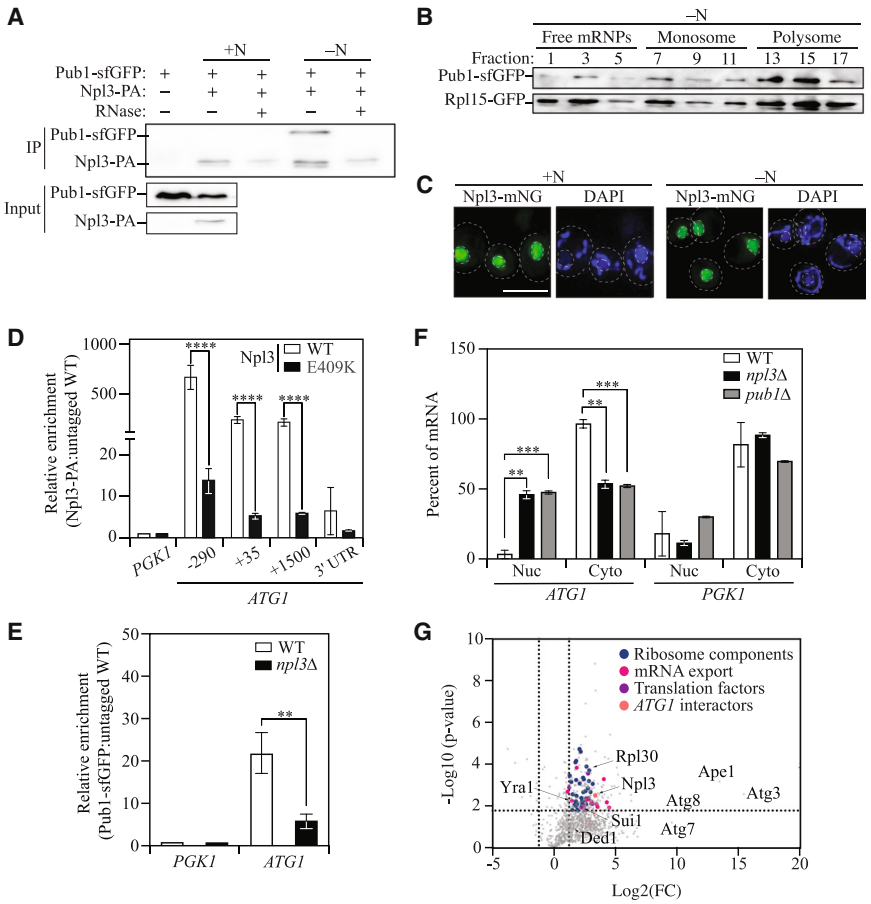

Figure 5. Pub1 links *ATG1* mRNA export and translation

(A) Npl3 and Pub1 interaction is RNA dependent. An Npl3-PA-tagged strain expressing a centromeric Pub1-sfGFP was subjected to nitrogen starvation and harvested after 4 h. Npl3-PA was affinity isolated using IgG Sepharose beads with or without RNase in +N and −N conditions and immunoblotted to determine Npl3 and Pub1 interaction. IP, immunoprecipitation.

(B) Pub1 localizes to different polysome compartments. Pub1-GFP (SPY069 + *ADH1p-PUB1-GFP*) and Rpl15-GFP (SPY069) strains were subjected to nitrogen starvation for 4 h, and equal fractions were collected by polysome profiling following ultracentrifugation in a sucrose gradient. Two consecutive fractions were combined, and proteins were analyzed by immunoblotting.

(C) Npl3 is predominantly localized to the nucleus. Npl3 was tagged with mNeonGreen (SPY067) and imaged under nitrogen-rich medium (+N) and nitrogen-starvation medium (−N) conditions. DAPI was used to stain DNA. Data represent 200 cells analyzed. Scale bar, 5 μm.

(D) Nuclear localization of Npl3 is required for it to bind to *ATG1* mRNA. RNA immunoprecipitation was performed using WT (untagged, SEY6210), Npl3-PA (SPY060), and Npl3^{E409K}-PA (SPY057) strains, and *ATG1* mRNA abundance was determined by RT-qPCR. Data represent three independent replicates, showing mean ± SD. ****$p < 0.0001$.

(E) Loss of Pub1 causes defects in *ATG1* mRNA export, similar to *npl3Δ*. WT (WLY176), *npl3Δ* (SPY077), and *pub1Δ* (SPY006) strains were subjected to nitrogen starvation for 4 h and fractionated to obtain nuclear and cytoplasmic fractions. *ATG1* abundance was determined by RT-qPCR. *PGK1* was used as a control. Two-way ANOVA was performed to determine statistical significance. ****$p = 0.0005$, ***$p = 0.0097$.

(F) Npl3 is required for Pub1-*ATG1* interaction during nitrogen starvation. A centromeric plasmid harboring Pub1-sfGFP was expressed in WT (WLY176) and *npl3Δ* (SPY077) strains and subjected to nitrogen starvation for 4 h, following which GFP-trap nanobeads were used to immunoprecipitate Pub1. Untagged WLY176 was used as a control. *ATG1* 3′ UTR abundance was determined by RT-qPCR. Data represent three independent biological replicates, showing mean ± SD. Two-way ANOVA was performed to determine statistical significance. **$p = 0.0095$.

(G) Pub1 interacts with ribosomal components and translation factors during nitrogen starvation: A Pub1-sfGFP-expressing strain and untagged WT (SEY6210) strain were subjected to nitrogen starvation for 4 h and immunoprecipitated using GFP-trap nanobeads. The interactome of Pub1 was identified by mass spectrometry. Data represent two independent replicates. Student's t test was used to determine statistical significance. A *p* value above 0.05 was considered significant.

Npl3 coordinates with Pub1 to export *ATG1* mRNA and recruit polysomes for translation

Our investigations into the *ATG1* mRNA interactome revealed Npl3 and Pub1 as post-transcriptional regulators. Previous high-throughput studies have shown that Npl3 interacts with Pub1.[24] This led us to ask whether Pub1 and Npl3 coordinate to enhance the translation of *ATG1* during nitrogen starvation. To examine this, we performed co-immunoprecipitation of Npl3 tagged with PA and determined the interaction of Pub1-tagged with sfGFP using immunoblot. Consistently, Npl3 interacted with Pub1 during nitrogen-starvation conditions but not in the presence of nitrogen, suggesting that this interaction was specific to autophagy-inducing conditions (Figure 5A). Furthermore, this interaction was dependent on RNA; RNase treatment of the cell lysate prior to immunoprecipitation essentially eliminated the interaction between the two proteins. This finding suggests that Npl3 and Pub1 might coordinate to post-transcriptionally regulate the *ATG1* transcript. Therefore, we tested whether the two proteins worked together in the polysome fraction. Toward this end, we tested the localization of Npl3 and Pub1 in the different fractions of free mRNPs, monosomes, and polysomes. Npl3 showed no enrichment in the monosome and polysome fractions (Figure S4A). In contrast, Pub1 interacted with both monosome and polysome fractions during nitrogen starvation, co-sedimenting with the cytosolic ribosome marker Rpl15 (Figure 5B). This finding suggests that Pub1 may have a more direct role in translational regulation of *ATG1*, while Npl3 may have an indirect role.

Considering that Npl3 did not interact with polysome components, we were interested to further dissect its role and localization in regulating *ATG1* at the post-transcriptional level. In line with this, we found that following growth in nutrient-rich conditions and

during nitrogen starvation, Npl3 was predominantly localized to the nucleus (Figure 5C). When we investigated the localization of Pub1 under the same conditions, we found that Pub1 was localized throughout the cell except in certain organelles such as the vacuole. Confocal imaging of Pub1-sfGFP along with a nuclear marker such as Nup116-mCherry showed that a subpopulation of Pub1 was present in the nucleus, suggesting that Pub1 acted as a nucleo-cytoplasmic shuttling protein while Npl3 was predominantly a nuclear protein (Figure S4B). Alternatively, we fractionated the cytoplasm and nucleus following nitrogen starvation and investigated the presence of Pub1 in the different fractions. We found that a small population of Pub1 was indeed found in the nucleus. Npl3, a nuclear protein, therefore interacted with the small population of Pub1 that was located in the nucleus.

To understand the importance of nuclear localization of Npl3, we used a point mutation that prevents nuclear shuttling. Previously, studies have shown that the point mutation E409K results in a protein predominantly localized to the cytosol.[25] This mutation is present in the region of Npl3 required for nuclear localization and results in a slower rate of import of Npl3 to the nucleus.[25] We constructed a strain containing this mutation and asked whether the E409K mutant showed defects in Atg1 expression. Indeed, $Npl3^{E409K}$ had lowered Atg1 protein during nitrogen starvation but not *ATG1* mRNA levels (Figures S4D–S4F). This defect resulted from the severe reduction in *ATG1* mRNA binding exhibited by the E409K mutant (Figure 5D). This finding suggests that nuclear localization of Npl3 is required for nitrogen-starvation-dependent upregulation of Atg1 protein expression, likely via the interaction with Pub1. Npl3 interacts with the transcription machinery and loads transcripts onto mRNPs responsible for transcript export, underscoring its pivotal role in the nucleus.[26] These findings suggest a mechanism whereby the surveillance protein Npl3 recruits Pub1 onto the *ATG1* transcript. Therefore, we asked whether the interaction of *ATG1* mRNA and Pub1 is dependent on the presence of Npl3. RNA immunoprecipitation of Pub1 in WT and *npl3Δ* backgrounds showed that the interaction of Pub1 and the *ATG1* 3′ UTR was severely reduced in the absence of *NPL3* (Figure 5E). Given that localization of Npl3 in the nucleus is critical for the Npl3-*ATG1* interaction and Npl3 is required for Pub1-*ATG1* interaction, we hypothesized that *ATG1* loading onto Pub1 by Npl3 is required to export *ATG1* transcript to the cytosol. Therefore, we asked whether *pub1Δ* cells also have an export defect of *ATG1* mRNA. We found that the percentage of mRNA in the nuclear fraction was much higher in the absence of Pub1 compared to the WT (Figure 5F), thus phenocopying *npl3Δ* cells.

An obvious question was, does Pub1 link *ATG1* mRNA export and translation? Pub1 interacts with polysomes, and several independent studies have shown that it also can interact with mRNA export proteins.[27] However, Pub1 is also a core stress granule component, with primary functions in the cytoplasm. Therefore, we wanted to determine all the interactions of Pub1 during nitrogen starvation and thus performed immunoprecipitation of Pub1-sfGFP followed by mass-spectrometry analysis to identify the factors that interact with Pub1 (Figure 5G). From this analysis, we confirmed the interaction of Pub1 with Npl3. Furthermore, we found that Pub1 interacted with several mRNA export proteins, along with Npl3. Notably, Pub1 interacted with Yra1 and Sem1, whose role in mRNA export from the nucleus has been long established.[28] We found that Pub1 bound to over 40 ribosome components, including large and small subunits, and interacted with translation factors such as Sui1 and Gcd1, involved in translation initiation, as well as Yef3, a translation elongation factor, thus suggesting that Pub1 indeed shuttles between the nucleus and the cytoplasm, linking mRNA export and translational machinery. Furthermore, Pub1 interacted with known RBPs that influence Atg1 protein levels, such as Dhh1, Pat1, Ded1, and Cdc33 (Data S3), confirming that Pub1 links the *ATG1* mRNA-protein interactome to the translational machinery and ribosome components to aid in translation. These results also suggest that Pub1 mediates two spatially separated processes of nuclear mRNP loading and cytoplasmic translation, providing a unifying mechanism of how previously identified interactors of *ATG1* help to deliver the transcript to translating ribosomes to enhance the Atg1 production needed to sustain starvation-dependent autophagy.

DISCUSSION

Recently, *ATG1* has emerged as a transcript regulated by multiple players in a nutrient-dependent manner. However, a comprehensive understanding of how multiple RBPs that interact with *ATG1* mRNA coordinate with each other to upregulate *ATG1* translation during nutrient starvation is an interesting question. We tried to answer this by utilizing *in vitro* transcribed *ATG1* 5′ UTR and 3′ UTR as bait, enabling the identification via mass spectrometry of proteins that interact with the *ATG1* UTRs. Screening the interactors enriched specifically in nitrogen starvation at the 5′ UTR and 3′ UTR, we discovered Npl3 and Pub1 as significant interacting partners of the *ATG1* transcript, which emerged as crucial promoters of autophagy and survival during nitrogen starvation. Npl3 is an mRNA surveillance protein involved in multiple events immediately after the transcription of messenger RNA. Previous reports have shown that Npl3 directly binds to RNA polymerase II components and facilitates transcription elongation.[17] Npl3 is then involved in ensuring proper processing of the newly synthesized transcript. For example, Npl3 monitors proper 5′ capping of the transcript, wherein uncapped mRNAs are subject to degradation by the nuclear exosome complex.[29] Evidence suggests that following proper processing, Npl3 recruits export-competent mRNPs. Our research reveals that deletion of *NPL3* leads to accumulation of the *ATG1* transcript in the nucleus, suggesting its role in the export of the transcript. The diminished autophagy activity and lowered cell survival in cells lacking *NPL3* are likely tied to the reduced translation of Atg1. However, the potential upregulation of other autophagy-related or regulatory proteins by Npl3 cannot be dismissed, as our study focused primarily on Atg1 regulation. We found that Npl3 directly binds to the *ATG1* transcript through its RRM motif, providing a new perspective on the role of Npl3 in autophagy regulation.

Furthermore, phosphorylation of Npl3 by Sky1 promotes Npl3 shuttling to the cytosol and mRNA dissociation.[30] However, our experiments showed that Sky1 did not affect Atg1 protein levels, suggesting that its role in the phosphorylation of Npl3 is not relevant to the export and translation of *ATG1* during nitrogen

starvation (Figure S5A). Consistent with this, we found that mutations that prevent proper nuclear localization of Npl3 led to a decrease in *ATG1* binding and expression with a concomitant decrease in autophagy. Therefore, while Npl3 is a known nuclear-to-cytosol shuttling protein, in the context of nutrient starvation it predominantly functions in the nucleus and facilitates priming of *ATG1* mRNA for export by Pub1.

Pub1 is an RBP known for its role in stabilizing stress-responsive mRNA and facilitating its translation; one such example is seen with Gcn4.[31] Here, we show that the deletion of *PUB1* does not affect the stability of *ATG1* mRNA; however, it directly affects its translation. Most importantly, we discovered that Npl3 binds to Pub1 in an RNA-dependent manner during nitrogen starvation. Using immunoprecipitation combined with mass spectrometry, we identified the interactors of Pub1 in nitrogen starvation. Pub1 interacts with export proteins such as Yra1 and Sem1, and likely escorts *ATG1* transcripts to the cytosol, where it interacts with several translation factors, including initiation and elongation factors, as well as more than 40 ribosomal components.[32,33] Additionally, we found that Mex67, Dbp2, and Nab2 interact with the *ATG1* 5′ UTR (Figure S5B). Dbp2 is required for the assembly of export components such as Nab2, Mex67, and Yra1 onto the RNA.[34] This complex may also include Pub1. However, the interaction of Pub1 and Nab2 is independent of RNA.[27] Interestingly, we showed that Pub1 also interacts with previously known *ATG1* interactors mentioned above, either directly or indirectly, via the *ATG1* transcript (Data S3). This finding suggests that the proteome components of the *ATG1* transcript function in close proximity to each other.

Crucially, we found this role to be conserved in humans as well via TIA1, a homolog of Pub1. Depletion of TIA1 results in the decrease of ULK1 protein levels and autophagy levels while not affecting the mRNA levels of *ULK1*. Finally, similar to Pub1, we found that TIA1 interacts with ULK1 at the 3′ UTR. Mutations in the *TIA1* gene have been linked to various neurodegenerative disorders. For instance, some studies have associated TIA1 mutations with amyotrophic lateral sclerosis and frontotemporal dementia, suggesting that these mutations may disrupt normal protein aggregation and RNA-metabolism processes in neurons.[35] The ability of TIA1 to influence autophagy, therefore, has significant implications for diseases in which autophagy is dysregulated. For instance, in neurodegenerative diseases, altered autophagy can contribute to the accumulation of toxic protein aggregates.[36] Modulating TIA1 function could potentially offer therapeutic strategies to enhance autophagy and mitigate disease progression.

Pub1 and its mammalian equivalent TIA1 interact with Sup35 and GSPT2, respectively.[37] Our study reveals that the *ATG1* 3′ UTR binds to Sup35 (Figure 3A), suggesting a novel mechanism whereby Pub1-Sup35 could facilitate local translation of autophagy-related proteins, akin to their proposed function in cytoskeleton integrity via tubulin translation.

While we provided novel insight into the role of Npl3 in regulating *ATG1* translation, specific to autophagy-inducing conditions, a question remains about the molecular trigger that allows for Npl3 to interact with *ATG1* mRNA upon the onset of nitrogen starvation and subsequent interaction with Pub1. Because we found that *sky1Δ* had no effect on Atg1 protein levels, we ruled out the possibility that Npl3 phosphorylation could be important. Alternatively, we found that total Npl3 protein levels significantly increased after 6 h of nitrogen starvation, albeit modestly (Figure S2E). The possibility of increase in protein levels leading to increasing in *ATG1* binding and Pub1 interaction cannot be ruled out and needs to be investigated further. With respect to Pub1, we found that it was phosphorylated in both +N and −N conditions (Figure S5C). This observation suggests the possibility that phosphorylation is important for its function but may not be a cue for nutrient-specific regulation. Both Npl3 and Pub1 are methylated by Hmt1, previously implicated in *ATG1* translation via Psp2.[11,12] Thus, it is possible that similar regulation occurs in the context of Npl3 and Pub1. This hypothesis needs further investigation.

Limitations of the study

Our study primarily relies on biochemical methods including RNA immunoprecipitation and co-immunoprecipitation to capture protein-RNA interaction and protein-protein interaction, respectively. While this is a standard assay in the field, it fails to differentiate between direct and indirect interactions. Therefore, to provide better insight into these interactions, *in vitro* experiments with purified proteins and *in vitro* transcribed mRNA are required. Next, we employed polysome profiling to determine the translation status of the *ATG1* transcript. The caveat with this experiment is that during nitrogen starvation the total number of polysomes is severely reduced, due to the block in global translation. Therefore, the yield of ribosomal fractions obtained is low, and further downstream analysis can further exacerbate technical artifacts. Additionally, this technique does not provide information regarding the region of the transcript that is translated. To circumvent these issues, a high-throughput approach such as ribosome profiling may be employed. We also provide insight into the nutrient-dependent role of Npl3 and Pub1; however, we did not identify an upstream cue such as a signaling protein or post-translational modification that drives the regulation. Further work will be needed to address this issue.

RESOURCE AVAILABILITY

Lead contact

Further information and requests for resources and reagents should be directed to and will be fulfilled by the lead contact, Prof. Daniel J. Klionsky (klionsky@umich.edu).

Materials availability

Plasmids and yeast strains will be made available upon request to the lead contact.

Data and code availability

- The mass spectrometry proteomics data have been deposited to the ProteomeXchange Consortium via the PRIDE partner repository with the dataset identifier PRIDE: PXD059054.
- No new code was generated in this paper. Please contact the corresponding author for any other data requirements.

ACKNOWLEDGMENTS

This work was supported by NIGMS grant GM131919 from the National Institutes of Health.

AUTHOR CONTRIBUTIONS

S.P.M. designed the project and performed most of the experiments. X.S. and D.T. performed mammalian experiments. S.M. and D.B. performed microscopy experiments. D.D. quantified Npl3 protein levels. Z.Y. constructed most of the Npl3 strains and first discovered its autophagy phenotype. S.P.M. drafted the manuscript. D.J.K. revised the manuscript and supervised the project.

DECLARATION OF INTERESTS

The authors declare no competing interests.

STAR★METHODS

Detailed methods are provided in the online version of this paper and include the following:

- KEY RESOURCES TABLE
- EXPERIMENTAL MODEL AND STUDY PARTICIPANTS
  - Yeast strains, media and growth conditions
  - Mammalian methods
- METHOD DETAILS
  - Plasmids
  - RNA methods
  - Protein methods
- QUANTIFICATION AND STATISTICAL ANALYSIS

SUPPLEMENTAL INFORMATION

Supplemental information can be found online at https://doi.org/10.1016/j.celrep.2025.115316.

Received: June 14, 2024
Revised: November 20, 2024
Accepted: January 23, 2025
Published: February 14, 2025; corrected online May 29, 2025

REFERENCES

1. Howell, J.J., and Manning, B.D. (2011). mTOR couples cellular nutrient sensing to organismal metabolic homeostasis. Trends Endocrinol. Metabol. *22*, 94–102. https://doi.org/10.1016/j.tem.2010.12.003.
2. Ryter, S.W., Cloonan, S.M., and Choi, A.M.K. (2013). Autophagy: a critical regulator of cellular metabolism and homeostasis. Mol. Cell. *36*, 7–16. https://doi.org/10.1007/s10059-013-0140-8.
3. Metur, S.P., and Klionsky, D.J. (2024). Nutrient-dependent signaling pathways that control autophagy in yeast. FEBS Lett. *598*, 32–47. https://doi.org/10.1002/1873-3468.14741.
4. Parzych, K.R., and Klionsky, D.J. (2014). An overview of autophagy: morphology, mechanism, and regulation. Antioxidants Redox Signal. *20*, 460–473. https://doi.org/10.1089/ars.2013.5371.
5. Abeliovich, H., and Klionsky, D.J. (2001). Autophagy in yeast: mechanistic insights and physiological function. Microbiol. Mol. Biol. Rev. *65*, 463–479, table of contents. https://doi.org/10.1128/MMBR.65.3.463-479.2001.
6. Metur, S.P., Lei, Y., Zhang, Z., and Klionsky, D.J. (2023). Regulation of autophagy gene expression and its implications in cancer. J. Cell Sci. *136*, jcs260631. https://doi.org/10.1242/jcs.260631.
7. Ma, Q., Long, S., Gan, Z., Tettamanti, G., Li, K., and Tian, L. (2022). Transcriptional and Post-Transcriptional Regulation of Autophagy. Cells *11*. Cells *11*, 441. https://doi.org/10.3390/cells11030441.
8. Noda, N.N., and Fujioka, Y. (2015). Atg1 family kinases in autophagy initiation. Cell. Mol. Life Sci. *72*, 3083–3096. https://doi.org/10.1007/s00018-015-1917-z.
9. Lahiri, V., Metur, S.P., Hu, Z., Song, X., Mari, M., Hawkins, W.D., Bhattarai, J., Delorme-Axford, E., Reggiori, F., Tang, D., et al. (2022). Post-transcriptional regulation of ATG1 is a critical node that modulates autophagy during distinct nutrient stresses. Autophagy *18*, 1694–1714. https://doi.org/10.1080/15548627.2021.1997305.
10. Lukong, K.E., Chang, K.W., Khandjian, E.W., and Richard, S. (2008). RNA-binding proteins in human genetic disease. Trends Genet. *24*, 416–425. https://doi.org/10.1016/j.tig.2008.05.004.
11. Liu, X., Yao, Z., Jin, M., Namkoong, S., Yin, Z., Lee, J.H., and Klionsky, D.J. (2019). Dhh1 promotes autophagy-related protein translation during nitrogen starvation. PLoS Biol. *17*, e3000219. https://doi.org/10.1371/journal.pbio.3000219.
12. Yin, Z., Liu, X., Ariosa, A., Huang, H., Jin, M., Karbstein, K., and Klionsky, D.J. (2019). Psp2, a novel regulator of autophagy that promotes autophagy-related protein translation. Cell Res. *29*, 994–1008. https://doi.org/10.1038/s41422-019-0246-4.
13. Nair, U., Thumm, M., Klionsky, D.J., and Krick, R. (2011). GFP-Atg8 protease protection as a tool to monitor autophagosome biogenesis. Autophagy *7*, 1546–1550. https://doi.org/10.4161/auto.7.12.18424.
14. Suzuki, S.W., Onodera, J., and Ohsumi, Y. (2011). Starvation induced cell death in autophagy-defective yeast mutants is caused by mitochondria dysfunction. PLoS One *6*, e17412. https://doi.org/10.1371/journal.pone.0017412.
15. Heyer, E.E., and Moore, M.J. (2016). Redefining the Translational Status of 80S Monosomes. Cell *164*, 757–769. https://doi.org/10.1016/j.cell.2016.01.003.
16. Schieweck, R., Ciccopiedi, G., Klau, K., and Popper, B. (2023). Monosomes buffer translational stress to allow for active ribosome elongation. Front. Mol. Biosci. *10*, 1158043. https://doi.org/10.3389/fmolb.2023.1158043.
17. Santos-Pereira, J.M., Herrero, A.B., Moreno, S., and Aguilera, A. (2014). Npl3, a new link between RNA-binding proteins and the maintenance of genome integrity. Cell Cycle *13*, 1524–1529. https://doi.org/10.4161/cc.28708.
18. Moursy, A., Cléry, A., Gerhardy, S., Betz, K.M., Rao, S., Mazur, J., Campagne, S., Beusch, I., Duszczyk, M.M., Robinson, M.D., et al. (2023). RNA recognition by Npl3p reveals U2 snRNA-binding compatible with a chaperone role during splicing. Nat. Commun. *14*, 7166. https://doi.org/10.1038/s41467-023-42962-4.
19. Gatica, D., Hu, G., Liu, X., Zhang, N., Williamson, P.R., and Klionsky, D.J. (2019). The Pat1-Lsm Complex Stabilizes ATG mRNA during Nitrogen Starvation-Induced Autophagy. Mol. Cell *73*, 314–324. https://doi.org/10.1016/j.molcel.2018.11.002.
20. Szostak, E., and Gebauer, F. (2013). Translational control by 3'-UTR-binding proteins. Brief. Funct. Genomics *12*, 58–65. https://doi.org/10.1093/bfgp/els056.
21. Delorme-Axford, E., Abernathy, E., Lennemann, N.J., Bernard, A., Ariosa, A., Coyne, C.B., Kirkegaard, K., and Klionsky, D.J. (2018). The exoribonuclease Xrn1 is a post-transcriptional negative regulator of autophagy. Autophagy *14*, 898–912. https://doi.org/10.1080/15548627.2018.1441648.
22. Hurt, E., Luo, M.J., Röther, S., Reed, R., and Strässer, K. (2004). Cotranscriptional recruitment of the serine-arginine-rich (SR)-like proteins Gbp2 and Hrb1 to nascent mRNA via the TREX complex. Proc. Natl. Acad. Sci. USA *101*, 1858–1862. https://doi.org/10.1073/pnas.0308663100.
23. Noda, T., and Klionsky, D.J. (2008). The quantitative Pho8Delta60 assay of nonspecific autophagy. Methods Enzymol. *451*, 33–42. https://doi.org/10.1016/S0076-6879(08)03203-5.
24. Gotor, N.L., Armaos, A., Calloni, G., Torrent Burgas, M., Vabulas, R.M., De Groot, N.S., and Tartaglia, G.G. (2020). RNA-binding and prion domains: the Yin and Yang of phase separation. Nucleic Acids Res. *48*, 9491–9504. https://doi.org/10.1093/nar/gkaa681.

25. Lei, E.P., Krebber, H., and Silver, P.A. (2001). Messenger RNAs are recruited for nuclear export during transcription. Genes Dev. *15*, 1771–1782. https://doi.org/10.1101/gad.892401.

26. Keil, P., Wulf, A., Kachariya, N., Reuscher, S., Hühn, K., Silbern, I., Altmüller, J., Keller, M., Stehle, R., Zarnack, K., et al. (2023). Npl3 functions in mRNP assembly by recruitment of mRNP components to the transcription site and their transfer onto the mRNA. Nucleic Acids Res. *51*, 831–851. https://doi.org/10.1093/nar/gkac1206.

27. Apponi, L.H., Kelly, S.M., Harreman, M.T., Lehner, A.N., Corbett, A.H., and Valentini, S.R. (2007). An interaction between two RNA binding proteins, Nab2 and Pub1, links mRNA processing/export and mRNA stability. Mol. Cell Biol. *27*, 6569–6579. https://doi.org/10.1128/MCB.00881-07.

28. MacKellar, A.L., and Greenleaf, A.L. (2011). Cotranscriptional association of mRNA export factor Yra1 with C-terminal domain of RNA polymerase II. J. Biol. Chem. *286*, 36385–36395. https://doi.org/10.1074/jbc.M111.268144.

29. Klama, S., Hirsch, A.G., Schneider, U.M., Zander, G., Seel, A., and Krebber, H. (2022). A guard protein mediated quality control mechanism monitors 5'-capping of pre-mRNAs. Nucleic Acids Res. *50*, 11301–11314. https://doi.org/10.1093/nar/gkac952.

30. Gilbert, W., Siebel, C.W., and Guthrie, C. (2001). Phosphorylation by Sky1p promotes Npl3p shuttling and mRNA dissociation. RNA *7*, 302–313. https://doi.org/10.1017/s1355838201002369.

31. Ruiz-Echevarria, M.J., and Peltz, S.W. (2000). The RNA binding protein Pub1 modulates the stability of transcripts containing upstream open reading frames. Cell *101*, 741–751. https://doi.org/10.1016/s0092-8674(00)80886-7.

32. Infantino, V., Tutucci, E., Yeh Martin, N., Zihlmann, A., Garcia-Molinero, V., Silvano, G., Palancade, B., and Stutz, F. (2019). The mRNA export adaptor Yra1 contributes to DNA double-strand break repair through its C-box domain. PLoS One *14*, e0206336. https://doi.org/10.1371/journal.pone.0206336.

33. Faza, M.B., Kemmler, S., Jimeno, S., González-Aguilera, C., Aguilera, A., Hurt, E., and Panse, V.G. (2009). Sem1 is a functional component of the nuclear pore complex-associated messenger RNA export machinery. J. Cell Biol. *184*, 833–846. https://doi.org/10.1083/jcb.200810059.

34. Ma, W.K., Cloutier, S.C., and Tran, E.J. (2013). The DEAD-box protein Dbp2 functions with the RNA-binding protein Yra1 to promote mRNP assembly. J. Mol. Biol. *425*, 3824–3838. https://doi.org/10.1016/j.jmb.2013.05.016.

35. Mackenzie, I.R., Nicholson, A.M., Sarkar, M., Messing, J., Purice, M.D., Pottier, C., Annu, K., Baker, M., Perkerson, R.B., Kurti, A., et al. (2017). TIA1 Mutations in Amyotrophic Lateral Sclerosis and Frontotemporal Dementia Promote Phase Separation and Alter Stress Granule Dynamics. Neuron *95*, 808–816. https://doi.org/10.1016/j.neuron.2017.07.025.

36. Park, H., Kang, J.H., and Lee, S. (2020). Autophagy in Neurodegenerative Diseases: A Hunter for Aggregates. Int. J. Mol. Sci. *21*, 3369. https://doi.org/10.3390/ijms21093369.

37. Li, X., Rayman, J.B., Kandel, E.R., and Derkatch, I.L. (2014). Functional role of Tia1/Pub1 and Sup35 prion domains: directing protein synthesis machinery to the tubulin cytoskeleton. Mol. Cell *55*, 305–318. https://doi.org/10.1016/j.molcel.2014.05.027.

38. Hu, G., McQuiston, T., Bernard, A., Park, Y.D., Qiu, J., Vural, A., Zhang, N., Waterman, S.R., Blewett, N.H., Myers, T.G., et al. (2015). A conserved mechanism of TOR-dependent RCK-mediated mRNA degradation regulates autophagy. Nat. Cell Biol. *17*, 930–942. https://doi.org/10.1038/ncb3189.

39. Kroschwald, S., Munder, M.C., Maharana, S., Franzmann, T.M., Richter, D., Ruer, M., Hyman, A.A., and Alberti, S. (2018). Different Material States of Pub1 Condensates Define Distinct Modes of Stress Adaptation and Recovery. Cell Rep. *23*, 3327–3339. https://doi.org/10.1016/j.celrep.2018.05.041.

40. Chomczynski, P., and Sacchi, N. (2006). The single-step method of RNA isolation by acid guanidinium thiocyanate-phenol-chloroform extraction: twenty-something years on. Nat. Protoc. *1*, 581–585. https://doi.org/10.1038/nprot.2006.83.

STAR★METHODS

KEY RESOURCES TABLE

REAGENT or RESOURCE	SOURCE	IDENTIFIER
Antibodies		
YFP	Clontech	632381; RRID:AB_2313808
Pgk1	Dr. Jeremy Thorner	N/A
Atg1	In house	N/A
Goat anti-Rabbit IgG, HRP	Fisher Scientific	ICN55676; RRID:AB_2334589
Rabbit anti-Mouse IgG, HRP	Jackson ImmunoResearch	315-035-003; RRID:AB_2340061
TIA1	Cell Signaling Technology	86050S; RRID:AB_2800070
ACTB	Cell Signaling Technology	3700; RRID:AB_2242334
SQSTM1	Cell Signaling Technology	88588, RRID:AB_2800125
LC3	Novus	Novus; RRID:AB_669581
ULK1	Cell Signaling Technology	8054S; RRID:AB_11178668
Chemicals, peptides, and recombinant proteins		
Triton X-100	Sigma Aldrich	X100-100ML
2-mercaptoethanol	Sigma Aldrich	M6250
cOmplete Mini EDTA-free protease inhibitor tablets	Roche	11836170001
Yeast extract	Formedium	YEA03
Peptone	Formedium	PEP03
Acrylamide	National Diagnostics	EC-890
IgG Sepharose 6 Fast Flow beads	Cytiva	17096901
Glycoblue	Thermo	Am9516
TURBO DNA-*free* kit	Fisher Scientific	AM1907
RNasin® PLUS RNase inhibitor	Fisher Scientific	PRN2615
Lipofectamine RNAiMAX	Invitrogen	13778030
PhosSTOP	Roche	Phoss-RO
GFP-trap nanobeads	Chromtek	gta
Critical commercial assays		
Pierce Magnetic RNA-Protein Pull-Down Kit	Thermo Fisher Scientific	20164
Nucleospin® RNA	Clontech	740955.250
BCA Protein assay	Fisher Scientific	PI23223, PI23224
Yeast Nuclei Isolation Kit	Abcam	ab206997
Experimental models: Cell lines		
Calu-1	ATCC	HTB-54
Deposited Data		
Mass spectrometry proteomics	ProteomeXchange Consortium	PXD059054
Experimental models: Organisms/strains		
S. cerevisiae: strain background SEY6210	See Table S2	N/A
Oligonucleotides		
Primers for RT-qPCR	Hu et al.[38]	N/A
siRNA universal negative control	Sigma	SIC001
TIA1 siRNA	Sigma	SASI-Hs01-0007018
Software and algorithms		
CFX Manager Software	Bio-Rad	N/A

EXPERIMENTAL MODEL AND STUDY PARTICIPANTS

Yeast strains, media and growth conditions

Yeast strains used in this study are listed in Table S1. Standard methods were used to generate gene deletions and tagging.

Yeast cells were grown in rich medium, YPD (1% yeast extract, 2% peptone and 2% glucose), until the OD_{600} reached 0.8–1.0. An appropriate volume of cells was collected by centrifugation, washed with water and transferred to nitrogen-starvation medium (−N; 0.17% yeast nitrogen base without ammonium sulfate or amino acid, 2% glucose) for the indicated times to induce starvation-dependent autophagy.

Mammalian methods

Calu-1 cells were cultured in Dulbecco's modified eagle's medium with 10% heat inactivated FBS, and antibiotics. TIA1 knockdown was performed by siRNA (Sigma, SASI-Hs01-0007018) using Lipofectamine RNAiMAX (Invitrogen, 13778030). For serum starvation, cells were transferred to Hanks' balanced salt solution for the specified time and collected for western blot. For RNA immunoprecipitation, we used a Magna RIP kit from Millipore Sigma.

METHOD DETAILS

Plasmids

pUC19-ATG1 5′ UTR has been described previously,[12] consisting of 500 base pairs (bp) upstream of the *ATG1* start codon. pUC19-ATG1 3′ UTR was constructed by amplifying the ~600 base pairs (bp) downstream of the *ATG1* stop codon and inserting the fragment into the pUC19 plasmid containing the T7 promoter. pUC19-PGK1 5′ UTR was constructed by amplifying 500 bp upstream of the *PGK1* start codon and inserting the fragment into the pUC19 plasmid. Centromeric Pub1sfGFP was described previously.[39]

RNA methods

mRNA invitro transcription

This method was carried out using the pUC19 plasmids as described above. Briefly, the plasmids were linearized using HindIII at 37°C for 2 h. One μg of linearized plasmid was then subject to *in vitro* transcription using the HiScribe T7 Quick High Yield RNA Synthesis Kit. The resulting RNA was purified using an RNA clean-up kit and quantified.

RNA labeling and affinity isolation

In vitro transcribed RNA (50 pmol) was used for a single labeling reaction with the desthiobiotin RNA labeling kit according to the manufacturer's instructions. The labeled RNA was then conjugated with streptavidin beads. Cells (200 OD_{600} units) grown in the appropriate medium were used for a single affinity-isolation reaction. Cells were lysed with polysome buffer (10 mM Tris-HCl, pH 7, 0.1 M NaCl, 30 mM $MgCl_2$, supplemented with a cOmplete protease inhibitor tablet and 40 units of RNase inhibitor and protein was quantified using the BCA assay. Equal amounts of protein were incubated with *ATG1* and *PGK1* RNA-conjugated beads at 4°C overnight on a rocking platform. The beads were then washed with wash buffer (provided in the kit) and sent to the Proteomics core in the Pathology Department, University of Michigan for on-beads digestion and protein identification. For analysis by immunoblotting, the beads were boiled in an equal volume of 2x MURB buffer, loaded onto SDS-PAGE gels and quantified by western blot.

Polysome profiling

All buffers were prepared using DEPC-treated water and cells and polysome fractions were kept on ice throughout the procedure. WT and mutant cells were grown in 125 mL of an appropriate rich medium to an OD_{600} of 0.8–1.0, and shifted to nitrogen-starvation medium. To the cells, 100 μg/mL cycloheximide was added and the culture was continuously shaken for 15 min at 250 rpm at 30°C. The cells were collected and lysed in a buffer containing 80 μg/mL cycloheximide, 200 μg/mL heparin, 0.2% DEPC, 10 mM Tris-HCl, pH 7.5, 0.1 M NaCl, 30 mM $MgCl_2$, and RNase inhibitor. The lysates were centrifuged at 16,000g for 10 min at 4°C and the supernatants collected. Sucrose gradients for ultracentrifugation were prepared a day in advance with 7%–47% sucrose solutions, including 20 mM Tris-HCl, pH 7.5, 140 mM KCl, 5 mM $MgCl_2$, 50 μg/mL cycloheximide, 0.1 mg/mL heparin, and 0.5 mM DTT. An equal amount of RNA across different experimental conditions was loaded onto the gradients and centrifuged at 35,000 rpm for 3 h at 4°C in an SW41Ti rotor. Following centrifugation, 500 μL fractions were collected in microcentrifuge tubes using a Brandel density gradient fractionator. Equal volumes of 100% ethanol, 0.2 ng/μL of *FLuc* mRNA and 5 μL of Glycoblue were added to each fraction and stored overnight at −80°C. The fractions were centrifuged at 16,000g for 15 min at 4°C. The resulting pellet was dissolved in 100 μL of water and RNA was extracted using a standard acid phenol and chloroform method,[40] followed by isopropanol and ethanol precipitation. The pellet was washed with 70% EtOH and air dried, then dissolved in 30 μL DEPC-treated water. A portion of this RNA (8 μL) was treated with TURBO DNase according to the manufacturer's instructions. A 9.6-μL aliquot of this reaction was used to convert to cDNA and the resulting cDNA was used to perform qPCR using a previously published protocol.[38] Each gene was normalized first to *FLuc* mRNA to account for differences in capture and precipitation of each sample. Next, the abundance of each mRNA in each fraction was normalized to the total amount of that mRNA on the gradient. These data were then used to determine the percentage abundance of RNA in each fraction.

RNA immunoprecipitation

The RNA immunoprecipitation protocol was adapted from earlier methods documented in several studies.[11,12] To explore the interaction between Npl3 and *ATG1* mRNA, strains with Npl3 tagged with PA in the genome and untagged control strains were grown to mid-log phase (~100 OD_{600} units of cells) and then subjected to nitrogen starvation for 3 h. Formaldehyde was at a final concentration of 0.8%, and the cultures were gently agitated for 10 min at room temperature to facilitate cross-linking. This reaction was quenched by adding glycine to a final concentration of 0.2 M and shaking for 5 more min. Afterward, the cultures were harvested, rinsed with PBS, and lysed in FA buffer (50 mM HEPES, pH 7.5, 150 mM NaCl, 1 mM EDTA, 1% Triton X-100, 0.1% sodium deoxycholate, 0.1% SDS) supplemented with 5 mM PMSF, a complete protease inhibitor cocktail tablet, PhosSTOP and RNasin PLUS RNase inhibitor. Cells were lysed by the addition of glass beads and mixing with a vortex at 4°C. The lysates were sonicated and subsequently divided into input and immunoprecipitation (IP) fractions. The IP fractions were incubated overnight with IgG Sepharose 6 Fast Flow beads at 4°C, while input samples were stored at −80°C. After multiple washes with FA buffer, IP fractions were eluted in RIP elution buffer (50 mM Tris-HCl, pH 7.5, 10 mM EDTA, 1% SDS) and treated with proteinase K in the presence of RNase inhibitor, at 42°C for 1 h followed by 65°C for 1 h to allow for the reversal of RNA-protein crosslinks. Samples were then subjected to acid phenol-chloroform extraction, and the aqueous phase was treated with sodium acetate, Glycoblue and ethanol to precipitate RNA. After incubation at −80°C, the RNA was pelleted, washed, dried, and resuspended in nuclease-free water. DNase treatment was used to remove any contaminating DNA, followed by RT-qPCR analysis as detailed in prior publications. For the analysis of Pub1-GFP interaction with *ATG1*, the same protocol was followed, except the lysates (after sonication and centrifugation) were incubated with GFP-trap nanobeads from Chromtek for 3 h before being washed with FA lysis buffer and proteinase K treatment as described above.

RNA extraction from nuclear and cytoplasmic fractions

Cells were grown in rich medium until they reached OD_{600} = 0.8 and shifted to nitrogen-starvation medium for 4 h. Cells (50 OD_{600} units) were collected, and the nuclear and cytoplasmic fractions were isolated using the Abcam Yeast Nuclei Isolation Kit. To the nuclear and cytoplasmic fractions, 2 pg of *FFLuc* mRNA were added as an internal control and total RNA was extracted using the standard acid phenol-chloroform method as described above.

Total RNA extraction, cDNA synthesis and qPCR

Total RNA was extracted using the Nucleo Spin RNA kit from Macherey Nagel, which includes a DNase treatment. One μg of total RNA was used to convert to cDNA using the High-capacity cDNA Reverse Transcription kit (Applied Biosystems). The transcript abundance in each sample was determined using methods and primers previously described. For comparison between wild type and mutants, the geometric mean of *Taf10*, *Tfc1* and *Cdc34*/*Ubc3* or *Sld3* was used as reference.

Protein methods

Protein extraction and immunoblotting

For analysis of Atg1 levels and other proteins, 1.2 OD_{600} units of yeast cells in the appropriate condition were precipitated with 10% trichloroacetic acid, followed by washing the cell pellet with acetone and air drying. The dried pellets were then lysed by adding glass beads in MURB buffer (50 mM sodium phosphate, pH 7.0, 25 mM MES, 1% SDS [w:v], 3 M urea, 1 mM NaN3, 1% β-mercaptoethanol, 0.01% bromophenol blue) and mixing on a vortex for 5 min. After lysis, samples were heated at 55°C for 15 min and then centrifuged at 10,000xg for 3 min to collect the supernatant for use in immunoblotting. Immunoblotting involved standard SDS-PAGE under denaturing conditions, followed by transfer using a Trans-Blot SD Semi-Dry Transfer Cell (Bio-Rad). The membrane was blocked with TBST containing 5% skim milk for 1 h and incubated with appropriate antibodies. Signal detection was performed using Clarity and Clarity Max ECL Western Blotting Substrates (Bio-Rad) and imaged with a ChemiDoc Touch Imaging System (Bio-Rad), then quantified using Bio-Rad image lab.

QUANTIFICATION AND STATISTICAL ANALYSIS

Statistical analysis was done using GraphPad Prism from 2 to 3 independent biological replicates using either Student's t test, one-way ANOVA or two-way ANOVA, corrected for multiple comparisons using Tukey's test. For all figures, a p value < 0.05 was considered significant.